

# LOW-POWER TEST OF BRIDGE COUPLER CONNECTED TO TANK IN DISK-AND-WASHER STRUCTURE FOR MUON ACCELERATION

A. Kondo\*, T. Iijima, K. Sumi, Y. Takeuchi, Nagoya University, Nagoya, Japan  
 E. Cicek, H. Ego, K. Futatsukawa, T. Mibe, Y. Nakazawa, M. Otani, M. Yoshida  
 High Energy Accelerator Research Organization, Tsukuba, Japan  
 Y. Kondo, M. Takatoshi, Japan Atomic Energy Agency, Tōkai Mura, Japan  
 Y. Iwashita, The University of Osaka, Osaka, Japan

## Abstract

A muon linear accelerator is under development at the Japan Proton Accelerator Research Complex (J-PARC) for precise measurement of the muon anomalous magnetic moment ( $g-2$ ) and search for the electric dipole moment (EDM). The disk-and-washer (DAW) structure is employed to accelerate muons from 30 % of the speed of light (kinetic energy = 4 MeV) to 70 % (40 MeV) at 1296 MHz. The muon DAW consists of tanks accelerating the muons and bridge couplers that couple the tanks and focus the beam using an internal quadrupole doublet. A bridge coupler prototype was fabricated and tested at low power. This low-power test focused on measuring resonant frequencies, Q-value, and electric field distribution. Furthermore, the bridge coupler prototype was connected to a tank prototype and tested at low power to understand the effects of the connection. This paper summarizes these results and discusses the prospects for actual machine production.

## INTRODUCTION

The muon anomalous magnetic moment ( $g-2$ ) and the electric dipole moment (EDM) are highly sensitive probes for physics beyond the Standard Model. Regarding the  $g-2$ , while recent lattice QCD calculations improve agreement with experimental results, a tension remains between lattice QCD-based and data-driven evaluations, requiring further investigation [1–3]. Furthermore, the observation of an EDM provides a stringent test for time-reversal symmetry violation [4].

At the Japan Proton Accelerator Research Complex (J-PARC), an experiment is being prepared to measure the muon  $g-2$  and search for the EDM using novel methods. One of the novel methods is accelerating muons by a linear accelerator (linac). The muon linac consists of four stages. A disk-and-washer (DAW) structure is employed as the third stage of the muon linac, designed to accelerate muons from 30 % of the speed of light (kinetic energy = 4 MeV) to 70 % (40 MeV) at 1296 MHz [5]. A DAW structure cavity is a type of coupled cavity linac (CCL) which consists of disks, washers, and supporting stems. It was first proposed in the 1970s [6] and later used for a proton accelerator [7]. It has a high shunt impedance for middle  $\beta$  and high electric field stability due to high coupling between accelerating cells and coupling cells.

The muon DAW consists of alternating accelerating tanks and bridge couplers. The bridge couplers electromagnetically couple the tanks and provide space for beam focusing using an internal quadrupole doublet. Figure 1 shows an overview of the muon DAW. For the bridge coupler, a coaxial-type one was selected to take full advantage of the high coupling of the DAW structure. Figure 2 illustrates the configurations of the tank-bridge coupler.

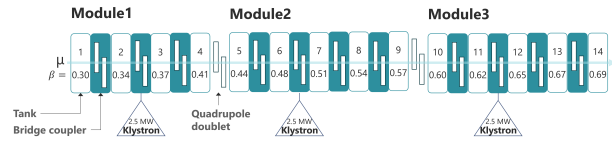


Figure 1: An overview of the muon DAW. The  $\beta$  shown in the figure represents the structure  $\beta$  ( $\beta_s$ ) of each tank. The cell length within each tank is fixed according to its  $\beta_s$ .

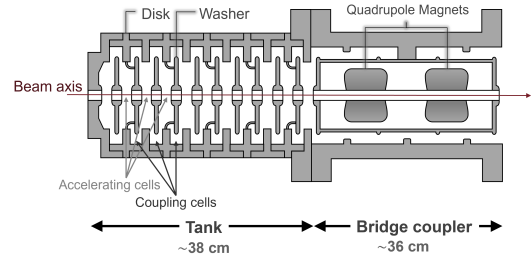


Figure 2: Cross-sectional view of the initial part of the muon DAW, cut vertically along the beam axis.

The development of the muon DAW began with the prototype fabrication of the first tank and bridge coupler. Because this initial section corresponds to the lowest particle velocity, it requires the narrowest accelerating gaps, presenting the most stringent fabrication challenges. A previous study reported the fabrication and performance evaluation of a tank prototype [8]. Also, a bridge coupler prototype was designed, fabricated, and was under evaluation [9]. This paper presents the low-power test results of this bridge coupler prototype, both individually and when connected to the tank prototype. The tests focused on measuring the resonant frequencies, Q-values, and electric field distributions.

## DESIGN

The design of the bridge coupler prototype is shown in Fig. 3 and Table 1. This design satisfies all RF require-

\* akondo@hepl.phys.nagoya-u.ac.jp

ments, which include an accelerating mode resonant frequency of  $1296.00 \pm 0.01$  MHz, a coupling mode frequency of  $1296 \pm 4$  MHz, and an electric field flatness of  $100 \pm 1\%$ , defined as the ratio of the downstream peak amplitude to the upstream peak amplitude of the on-axis electric field. The detailed design process and final parameters are described in [9]. However, as a simplified prototype (shown in Fig. 4), it differs from the final production version in its material composition and omits the internal quadrupole magnet.

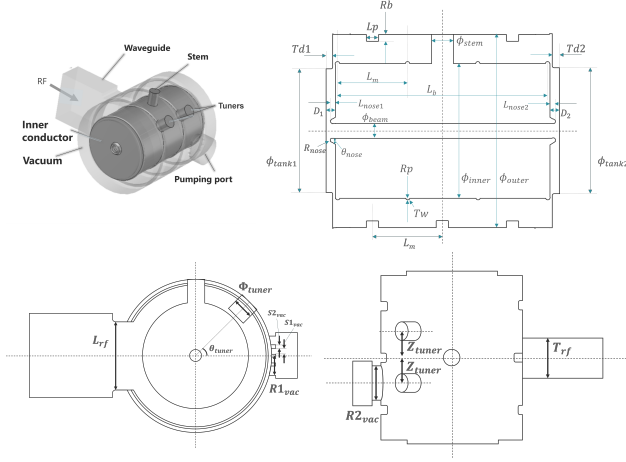


Figure 3: Cavity design. Top left: overall view. Top right: longitudinal cross-section. Bottom left: transverse cross-section. Bottom right: top view.

Table 1: Dimensions of the Most Upstream Bridge Coupler in the Final Design

Parameter	Value	Parameter	Value
$L_b$	329.197 mm	$L_m$	109.732 mm
$\phi_{stem}$	34 mm	$\phi_{inner}$	210 mm
$\phi_{outer}$	300 mm	$\phi_{beam}$	23.5 mm
$\phi_{tank1}$	194.6284 mm	$\phi_{tank2}$	196.7722 mm
$R_p$	2.82 mm	$L_p$	19.299 mm
$T_w$	Radius: 3.5 mm	$R_b$	10.69 mm
$Td1$	9.64945 mm	$Td2$	11.57 mm
$D_1$	13.6 mm	$D_2$	15.9 mm
$R_{nose}$	2.6 mm	$\theta_{nose}$	$30^\circ$
$L_{nose1}$	8.304 mm	$L_{nose2}$	9.397 mm
$L_{rf}$	134 mm	$T_{rf}$	82.55 mm
$\Phi_{tuner}$	40 mm	$\theta_{tuner}$	$45^\circ$
$Z_{tuner}$	54.8656 mm	$S1_{vac}$	17 mm
$S2_{vac}$	6 mm	$R1_{vac}$	46 mm
$R2_{vac}$	39 mm		

## LOW-POWER TEST

In the low-power test, the accelerating mode resonant frequency, Q-value, and electric field distribution of the bridge coupler prototype were measured. The coupling mode frequency could not be measured due to practical limitations in realizing the required boundary conditions in the actual apparatus. A Vector Network Analyzer was used for the

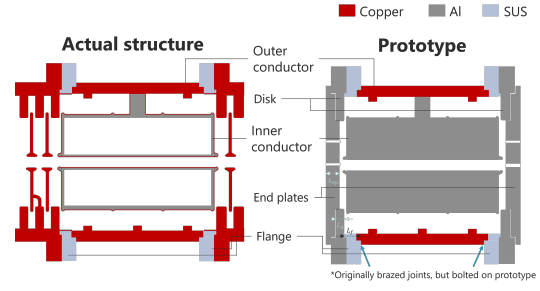


Figure 4: Bridge coupler prototype. The dimensions are  $L_{ep} = 33$  mm,  $L_d = 10$  mm, and  $L_f = 26.2$  mm.

measurements, and the electric field distribution was evaluated using the bead-pull method [10]. The experimental results were compared with simulations that incorporated the actual measurement conditions, including the presence of antennas and other measurement components.

The measurement results are summarized in Table 2 and Fig. 5. The measured resonant frequency of the accelerating mode deviated from the target, failing to meet the requirement of  $\pm 0.01$  MHz. Furthermore, the measured unloaded Q-value ( $Q_0$ ) was significantly low, reaching only about 35% of the simulated value. However, the measured electric field flatness showed good agreement with the simulation results.

Table 2: Comparison of measured and simulated RF properties. The measured values are corrected to the actual operating environment (vacuum, 30 °C). Measurement uncertainties represent the standard deviation of multiple measurements (omitted for single measurements). Simulation uncertainties are evaluated based on mesh convergence in CST Studio Suite [11].

Parameter	Measured	Simulated
Resonant frequency [MHz]	$1294.7 \pm 0.1$	$1295.6 \pm 0.2$
$Q_0$	3951	$6184 \pm 5$
Electric field flatness [%]	$101.4 \pm 0.4$	$101.6 \pm 0.5$

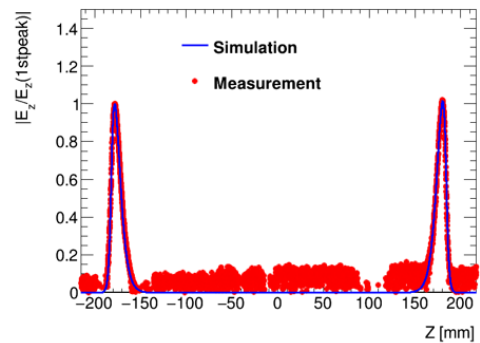


Figure 5: Electric field distribution along the beam axis.

## DISCUSSION AND ADDITIONAL TESTS

### Accelerating Mode Frequency and Tuner Study

The measured accelerating mode frequency was 0.9 MHz lower than the simulated value. To verify whether this dis-

crepancy could be compensated, a sensitivity study was conducted using a simplified tuner in the coupled setup with a tank prototype (1 unit) on the upstream side. Although this temporary tuner lacks a precise adjustment mechanism, it allows for an insertion length of up to 15 mm. The frequency shift measured over the tuner insertion range of 10 mm to 15 mm, where the tuner response is assumed to be sufficiently linear, agrees with the simulated frequency shift within 16 % [12]. This level of agreement validates the accuracy of the model.

Based on this validation, we evaluated the frequency correction capability for the final production version. The current design incorporates two tuners, each insertable up to 40 mm, providing a simulated total tuning range of 2.6 MHz. Given the demonstrated accuracy of the simulation model, the observed 0.9 MHz deviation is well within the compensation range of the production tuners.

### *Analysis of $Q$ -value Degradation*

The measured  $Q_0$  was low, reaching only about 35 % of the simulated value. A probable cause is imperfect contact between the assembled structures, which disrupts the flow of surface currents and consequently increases losses. However, the exact cause has not yet been definitively identified. Therefore, further investigation into the  $Q_0$  degradation is required, alongside a re-evaluation using a model that reflects the final production specifications.

### *Adjustment of Electric Field Flatness*

The electric field flatness is highly sensitive to the axial position of the inner conductor; simulations predict a sensitivity of up to 34 % per 1 mm. To experimentally verify this relationship, measurements were performed by slightly varying the conductor’s axial position, with displacements precisely tracked using a coordinate measuring machine (CMM). Through this sensitivity evaluation, we confirmed that the electric field flatness can be controlled by adjusting the inner conductor’s axial position, successfully tuning the measured field flatness to match the simulated values within the range of uncertainty. However, achieving this alignment through manual iteration is impractical for the final version due to reproducibility issues and the effort required for disassembly. Therefore, a precise axial positioning mechanism for the inner conductor will be implemented in the actual cavity to establish a reliable tuning method.

### *Connecting to the Tank*

Furthermore, the same parameters were measured with the bridge coupler connected to a tank prototype (1 unit) on the upstream side and an endcell (a terminating plate simulating a tank shape) on the downstream side. The results are summarized in Table 3. Although a mode corresponding to the accelerating mode was identified, its resonant frequency did not meet the requirement, and the  $Q_0$  exhibited a further decrease. Nevertheless, consistent with the measurement of the isolated bridge coupler, the electric field distribution was confirmed to be flat.

Table 3: Comparison of Measured and Simulated RF Properties With the Tank Connection

Parameter	Measured	Simulated
Resonant frequency [MHz]	1297.3	1295.7 ± 0.1
$Q_0$	269.29	10 271 ± 9
Field flatness [%]	98.7 ± 1.1	99.8 ± 0.1

However, it should be noted that the tank prototype used in this setup had known fabrication deviations, which had already resulted in a resonant frequency shift and a degraded  $Q_0$  during its standalone measurements [12]. Consequently, the results of the combined setup likely reflect a convolution of the connection effects and the inherent suboptimal performance of the tank itself. Future work will involve these measurements with a tank that fully meets the design specifications to accurately assess the impact of the tank connection on the bridge coupler’s performance.

## CONCLUSION

This study demonstrated the fabrication of a bridge coupler prototype capable of exciting the required accelerating mode. Based on the low-power test results, several key prospects for the final production version were identified. The measured resonant frequency and  $Q_0$  deviated from the simulated values. The frequency is expected to be corrected to the target value by implementing tuners with precise adjustment mechanisms. To address the  $Q_0$  degradation, further investigation and re-evaluation using a model reflecting the final specifications are required. Furthermore, while the electric field flatness can be controlled by adjusting the inner conductor’s axial position, a precise positioning mechanism will be introduced in the actual cavity to improve reproducibility. Finally, combined tests with a tank prototype excited the accelerating mode, but future evaluations must utilize a tank with verified RF performance to accurately assess the connection’s impact.

## ACKNOWLEDGMENTS

This work is supported by JSPS KAKENHI Grant Numbers 22H00141, 21H05088, 25H00401, 25H01295, the JST FOREST Program (Grant Number JPMJFR2120), the Toray Science and Technology Award and Research Grant, and the natural science grant of the Mitsubishi Foundation, Support for academic and research activities from Sumitomo Electric Group CSR Foundation, and Support for academic and research activities from CASIO SCIENCE PROMOTION FOUNDATION. We express our appreciation to Mitsubishi Heavy Industries, Ltd., which fabricated the bridge coupler.

## REFERENCES

- [1] D. P. Aguillard *et al.*, “Measurement of the positive muon anomalous magnetic moment to 127 ppb”, *Phys. Rev. Lett.*, vol. 135, no. 10, p. 101802, Sep. 2025.  
[doi:10.1103/7c1f-sm2v](https://doi.org/10.1103/7c1f-sm2v)

- [2] T. Aoyama *et al.*, “The anomalous magnetic moment of the muon in the Standard Model”, *Phys. Rep.*, vol. 887, pp. 1–166, Dec. 2020. doi:10.1016/j.physrep.2020.07.006
- [3] R. Aliberti *et al.*, “The anomalous magnetic moment of the muon in the standard model: an update”, *Phys. Rep.*, vol. 1143, pp. 1–158, Nov. 2025. doi:10.1016/j.physrep.2025.08.002
- [4] Y. Yamaguchi and N. Yamanaka, “Large long-distance contributions to the electric dipole moments of charged leptons in the Standard Model”, *Phys. Rev. Lett.*, vol. 125, no. 24, Dec. 2020. doi:10.1103/physrevlett.125.241802
- [5] M. Otani *et al.*, “Disk and washer coupled cavity linac design and cold-model for muon linac”, *J. Phys.: Conf. Ser.*, vol. 1350, p. 012097, Nov. 2019. doi:10.1088/1742-6596/1350/1/012097
- [6] V. G. Andreev *et al.*, “Study of high-energy proton linac structures”, in *Proc. LINAC’72*, Los Alamos, NM, USA, Oct. 1972, paper E04, p. 114.
- [7] S. K. Esin *et al.*, “The disk and washer structure for moscow meson factory linac”, in *Proc. LINAC’88*, Williamsburg, Virginia, USA, Oct. 1988, paper TH3-53, p. 657.
- [8] Y. Takeuchi *et al.*, “Fabrication and low-power test of disk-and-washer cavity for muon acceleration”, in *Proc. IPAC’22*, Bangkok, Thailand, Jun. 2022, pp. 1534–1537. doi:10.18429/JACoW-IPAC2022-TUPOMS046
- [9] A. Kondo *et al.*, “Low-power test of bridge coupler in disk-and-washer structure for muon acceleration”, *J. Phys.: Conf. Ser.*, vol. 3094, no. 1, p. 012025, Sep. 2025. doi:10.1088/1742-6596/3094/1/012025
- [10] T. P. Wangler, *RF linear accelerators*. Weinheim: Wiley-VCH Verlag GmbH & Co. KGaA, 2008.
- [11] CST STUDIO SUITE. <https://www.3ds.com/ja/products/simulia/cst-studio-suite>
- [12] A. Kondo, “Development of a bridge coupler for high-efficiency muon acceleration toward the muon  $g-2$ /EDM precision measurement/search (in japanese)”, MA thesis, Nagoya University, Nagoya, Japan, Mar. 2026.